

## Dynamics of hydrogen dissociation at the sulfur-covered Pd(100) surface

Axel Groß

*Physik-Department T30, Technische Universität München, D-85747 Garching, Germany*

Matthias Scheffler

*Fritz-Haber-Institut der Max-Planck-Gesellschaft, Faradayweg 4-6, D-14195 Berlin-Dahlem, Germany*

(Received 6 October 1999)

We report calculations of the dissociative adsorption and associative desorption of  $H_2$  at Pd(100) covered with 1/4 monolayer of sulfur using quantum dynamics as well as molecular dynamics and taking all six degrees of freedom of the two H atoms fully into account. The potential energy surface (PES) has been derived from density-functional theory calculations. The absolute value of the calculated sticking coefficient turns out to be at variance with a molecular beam experiment. However, the relative change of the sticking coefficient as a function of the angle of incidence as well as the mean kinetic energy and the rotational alignment of desorbing hydrogen molecules agree quite well with the experiment. This indicates that the calculated PES reproduces the most favorable reaction path, but that in the experiment the sulfur adlayer was probably not very well ordered.

### I. INTRODUCTION

An understanding of the electronic and geometric factors that promote or poison chemical reactions on surfaces is crucial for, e.g., designing better catalysts in heterogeneous catalysis. Recently, poisoning of car exhaust catalysts by sulfur that is still present in the gasoline has drawn a lot of attention. A number of surface science studies—experimental<sup>1-3</sup> as well as theoretical<sup>4-9</sup>—have been devoted to the promoting or poisoning effects of coadsorbates. The theoretical efforts were based on total-energy calculations in order to determine the change of dissociation energy barriers of the potential energy surface due to the presence of the promoting or poisoning coadsorbate. Several general reactivity concepts have been developed in order to analyze the factors that lead to the change of barriers. These concepts focused on the density of states,<sup>4,10</sup> on the polarizability of the surface,<sup>11</sup> or on electrostatic effects.<sup>12</sup>

However, knowledge about the energy barrier distribution is usually not sufficient to allow a quantitative comparison with experiment. In an experiment the reaction barriers or the potential energy surface are in general not directly measured but rather reaction rates and probabilities of the reactants moving on the potential energy surface (PES). Recently, it has been shown, e.g., that the sticking probability of  $H_2$  on Pd(100) and Rh(100) is quite similar at low kinetic energies although the underlying potential energy surfaces are rather different.<sup>13</sup> This fact is due to purely dynamical effects of the reactants moving on the relevant PES. Hence, in order to check the accuracy of calculations quantitatively, the actual dynamics of the reactants have to be calculated.<sup>14</sup>

Recently we have theoretically studied the dynamics of the adsorption of  $H_2$  on the  $(2 \times 2)$  sulfur-covered Pd(100) surface.<sup>15</sup> As far as the absolute value of the sticking coefficient is concerned, we obtained large differences between the theoretical results and the results of the molecular beam experiment of Rendulic *et al.*<sup>1</sup> At low kinetic energies, i.e., below the theoretical minimum barrier height  $E_b = 0.09$  eV,

the experiment yielded sticking coefficients on the order of 0.5% while in the calculations the sticking coefficients in this tunneling regime were exponentially small (below  $10^{-4}$ ). On the other hand, for energies above  $E_b$  the theoretical sticking coefficients turned out to be larger than the experimental results by a factor of up to 3 or 4. The experimental sticking curve exhibited a hump close to  $E_b$  which seemed to be the only agreement between theory and experiment.

In order to analyze the reason for this discrepancy between theory and experiment we have extended our theoretical study of hydrogen dissociation on the sulfur-covered Pd(100) surface. We have determined the dependence of the sticking probability on internal molecular degrees of freedom in great detail by performing *ab initio* quantum and classical molecular dynamics simulations in which all six hydrogen degrees of freedom are taken fully into account. We have compared the relative change of the sticking probability as a function of the angle of incidence with the experiment.<sup>1</sup> Furthermore, sticking probabilities can be directly converted into desorption distributions because desorption is related to adsorption via time reversal. We have calculated the mean kinetic energy in desorption, which had already been measured.<sup>16</sup> In addition, we have compared the calculated rotational alignment in desorption with a very recent experiment.<sup>17</sup>

In fact, our results compare quite well with the experimental results, as far as the dependence of the results on internal degrees of freedom and the angle of incidence is concerned. While the absolute value of the sticking coefficient in experiments corresponds to an average over many surface sites, the relative change of the sticking coefficient as a function of internal degrees of freedom of the molecular beam yields a more local information about the potential energy surface close to the most probable reaction path. The dependence of the sticking probability on the angle of incidence is related to the variation of the barrier distribution within the surface unit cell of the most favorable reaction path, while the dependence of the sticking probability on the

rotational motion of the molecules reflects the anisotropy of the PES. This indicates that the minimum energy barrier as well as the corrugation and anisotropy of the potential energy surface close to the most favorable reaction path are well reproduced by the calculations. We speculate that the discrepancy between theory and the molecular beam experiment could be due to the fact that in the experiment the sulfur adlayer might not be very well ordered. For such a situation, the comparison between experiment and a theory that assumes a perfectly well-ordered surface does not provide unambiguous information.

This paper is structured as follows. After this introduction a brief discussion of the theoretical methods is presented. Then we briefly review the experimental situation; in particular, we focus on the preparation of the sulfur adlayer. In the main section of the paper we discuss our results, first for hydrogen adsorption and then for desorption. The paper ends with some concluding remarks.

## II. COMPUTATIONAL DETAILS

The six-dimensional PES of the system  $\text{H}_2/\text{S}(2\times 2)/\text{Pd}(100)$  has been determined in great detail<sup>7</sup> using density-functional theory (DFT) together with the generalized gradient approximation (GGA).<sup>18</sup> The discrete *ab initio* data have been used to adjust the parameters of a continuous analytical representation. The particular form of this representation is also given in Ref. 7.

On this six-dimensional PES we have performed dynamical calculations taking into account all hydrogen degrees of freedom either by solving the time-independent Schrödinger equation within a coupled-channel scheme<sup>19</sup> or by integrating the classical equation of motion with the Bulirsch-Stoer method with a variable time step.<sup>20</sup> The computational methods for the dynamical calculations have been described in detail in Ref. 21. We point out that in all our calculations we have kept the substrate fixed, an approximation which is usually made in the simulation of hydrogen dissociative adsorption on metal surfaces<sup>22</sup> and which is justified by the large mass mismatch between the hydrogen and the substrate atoms. Hence no energy transfer to the substrate is considered in our calculations. Thus only the initial bond-breaking process is described, but not the dissipation of the kinetic energy of the atomic fragments to the surface. This hardly influences the calculated sticking probabilities, which are almost entirely determined by the initial dissociation probability on the surface. The hydrogen dissociation is considered to be complete if the hydrogen atoms are further apart than 2.5 Å on the surface.

The convergence of the quantum dynamical results with respect to the basis set has been carefully tested. Most results presented here have been obtained using rotational eigenfunctions with rotational quantum numbers up to  $j_{\text{max}}=8$ , vibrational eigenfunctions with vibrational quantum numbers up to  $v_{\text{max}}=2$ , and parallel momentum states with maximum parallel momentum  $p_{\text{max}}=10\hbar G$  with  $G=2\pi/a$ , where  $a$  is the lattice constant of the surface unit cell,  $a=5.5$  Å. These calculations were partly done in a massively parallel fashion on a Cray T3E. Due to the use of curvilinear coordinates in the quantum dynamics a nonsymmetric matrix has to be diagonalized. In the massively parallel implementation this is

done by using a second-order diagonalization scheme. For details, see Ref. 23.

## III. EXPERIMENTAL SITUATION

The sulfur adlayers on the Pd(100) surfaces used in the experiments that we refer to in this paper were prepared by either sulfur segregation from the bulk<sup>1,16</sup> or dissociative adsorption of  $\text{H}_2\text{S}$ .<sup>2,16,17</sup> While Rendulic *et al.* measured the sulfur coverage just through the ratio of the Auger peaks  $S_{152}/\text{Pd}_{330}$ ,<sup>1</sup> the other groups also used low-energy electron diffraction (LEED) to monitor the sulfur adlayer. On Pd(100) sulfur-induced  $p(2\times 2)$  and  $c(2\times 2)$  LEED patterns can be observed;<sup>2,24</sup> however, Comsa *et al.*<sup>16</sup> and Rutkowski *et al.*<sup>17</sup> report only the observation of  $c(2\times 2)$  patterns. Apparently the sulfur-induced  $p(2\times 2)$  structure on Pd(100) is hard to resolve by LEED.<sup>25</sup> Interestingly, for saturation coverage of sulfur on Pd(100) different values for the Auger peak ratio  $S_{152}/\text{Pd}_{330}$  have been reported: 0.35,<sup>16</sup> 0.54,<sup>1</sup> and 0.75.<sup>17</sup> This variation might be caused by differences in the kinetic energy of the primary electrons or in the angle of incidence.<sup>25</sup>

The molecular beam data of Rendulic *et al.*<sup>1</sup> show a non-vanishing hydrogen sticking coefficient at the sulfur-covered Pd(100) surface in the low-kinetic-energy limit. This suggests the existence of reactive sites at the sulfur-covered surface to which the  $\text{H}_2$  molecules are effectively steered.<sup>26</sup> At higher kinetic energies the experimental sticking coefficient is much smaller than the calculated one.<sup>15</sup> It has been proposed that this discrepancy might be due to the presence of subsurface sulfur in the experimental sample.<sup>15</sup> The calculations assumed a perfectly ordered  $(2\times 2)$  sulfur-covered Pd(100) surface without any subsurface sulfur; however, these subsurface species might well have been present in the experiment, assuming that the segregation of bulk sulfur to the surface was not fully complete.

Burke and Madix showed in an independent experiment<sup>2</sup> that for sulfur coverages above  $\Theta_{\text{S}}=0.28$  no hydrogen dissociation on Pd(100) is possible, while Rendulic *et al.* observed hydrogen dissociation at a sulfur-covered Pd(100) surface up to the maximum sulfur coverage of  $\Theta_{\text{S}}=0.5$ . However, Burke and Madix prepared the sulfur adlayer by  $\text{H}_2\text{S}$  dissociation while Rendulic *et al.* used segregation from the bulk. The results of Burke and Madix are actually in agreement with the DFT calculations,<sup>7</sup> which suggest that hydrogen dissociation at the  $c(2\times 2)$  sulfur-covered Pd(100) surface corresponding to a sulfur coverage of  $\Theta_{\text{S}}=0.5$  should be hindered by energetic barriers larger than 2 eV, so that hydrogen dissociation at this surface is completely suppressed at thermal energies.

It is certainly fair to say that some uncertainties remain as far as the preparation of a well-defined sulfur adlayer on Pd(100) in the experiments is concerned.

## IV. RESULTS AND DISCUSSION

### A. Dependence of the sticking probability on internal molecular degrees of freedom

The sticking probability as a function of the kinetic energy for a  $\text{H}_2$  beam under normal incidence on a  $\text{S}(2\times 2)/\text{Pd}(100)$  surface is plotted in Fig. 1. The results are shown for different initial states of the molecule. For the

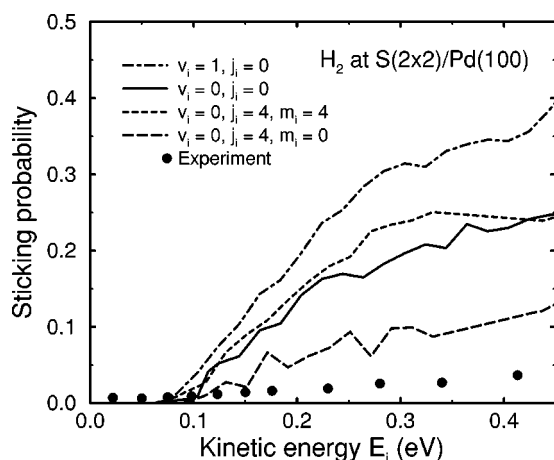


FIG. 1. Quantum sticking probability versus kinetic energy for a  $H_2$  beam under normal incidence on a  $S(2 \times 2)/Pd(100)$  surface for different initial rotational states with rotational quantum number  $j$  and azimuthal quantum number  $m_j$  and different initial vibrational states  $v$  (see legend). The experimental results from a molecular beam experiment (Ref. 1) are also shown (filled dots).

sake of completeness we briefly refer to the results for initially nonrotating molecules which have already been published.<sup>15</sup> The solid line corresponds to molecules initially in the vibrational and rotational ground state. As we have already pointed out in the Introduction, for energies above the minimum barrier height these sticking probabilities are larger by a factor of 3 or 4 compared to experiment.<sup>1</sup> On the other hand, at very low kinetic energies the experimental sticking coefficient is approximately independent of the kinetic energy at a value of about 0.005, while the calculated sticking probability becomes exponentially small, below  $10^{-4}$ .

Interestingly enough, initial vibrational excitation of the molecules enhances the sticking probability. This is surprising considering the fact that the system  $H_2/S(2 \times 2)/Pd(100)$  is an early barrier system,<sup>7</sup> i.e., the minimum barrier is at a position where the molecular bond is not significantly elongated. In such a situation it has usually been argued that the vibrational motion does not couple to the sticking probability.<sup>22,27</sup> However, not all dissociating molecules propagate across the minimum barrier position. Some cross the barrier to dissociation at sites in the unit cell where there is a later barrier,<sup>15</sup> for example at the bridge site between two adjacent Pd atoms.<sup>7</sup> The distribution of early and late barriers leads to a net vibrational effect in the sticking probability.<sup>15</sup>

We now turn to the dependence of the sticking probability on the rotational state. Rotating molecules are characterized by the rotational quantum number  $j$  and the azimuthal quantum number  $m_j$ , which indicates the orientation of the rotational axis. Rotating molecules with  $m_j=j$ , so-called helicopter molecules, have their rotational axis preferentially oriented perpendicular to the surface, while the rotational axis of cartwheel molecules with  $m_j=0$  is oriented preferentially parallel to the surface. Figure 1 shows that for  $j=4$  the sticking probability for molecules rotating in the helicopter fashion is almost the same as for nonrotating molecules, even a little bit larger. On the other hand, the sticking probability for the cartwheeling molecules is strongly lowered compared to the nonrotating molecules.

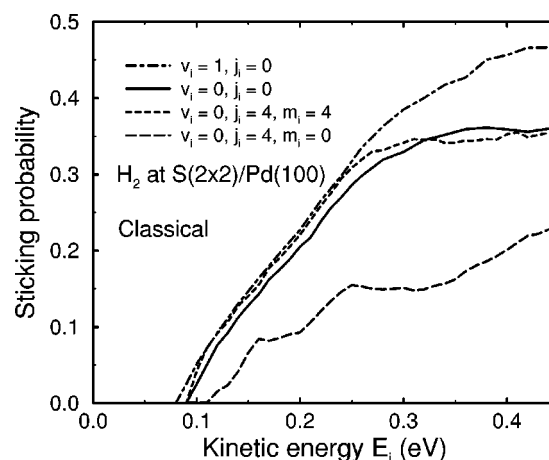


FIG. 2. Classical sticking probability versus kinetic energy for a  $H_2$  beam under normal incidence on a  $S(2 \times 2)/Pd(100)$  surface for different initial molecular states. The notation is equivalent to Fig. 1.

These results are a consequence of the anisotropy of the PES. Rapidly rotating molecules will rotate out of a favorable orientation for dissociation and thus show a smaller sticking probability than nonrotating molecules. This mechanism is called rotational hindering.<sup>22</sup> Moreover, only molecules with their axis parallel to the surface can dissociate. Cartwheeling molecules have a high probability of hitting the surface in an upright position, which further suppresses their sticking probability. On the other hand, molecules rotating in the helicopter fashion with  $j=m_j$  have their molecular axis already in the favorable orientation parallel to the surface. This steric effect can cancel or even overcompensate the rotational hindering, as the results for the molecules initially rotating with  $j=m_j=4$  in Fig. 1 demonstrate.

Experimentally it is hard to align a molecular hydrogen beam. Still, one can check these steric effects in adsorption by looking at the time-reverse process, desorption of hydrogen molecules. We will address this issue in Sec. IV C and show that these steric effects are indeed confirmed experimentally.

We now focus on the sticking probabilities obtained by classical molecular dynamics calculations. In Fig. 2 we have plotted the classical sticking probabilities for different initial “states.” These probabilities are obtained by summing up over trajectories whose initial conditions correspond to the distribution over particular quantum states. Exactly the same states have been considered as in Fig. 1. It should be noted, however, that we have not considered the vibrational zero-point energy of  $H_2$  in the initial conditions, i.e., the results in Fig. 2 correspond to classical trajectory calculations and *not* to so-called quasiclassical trajectory calculations. For hydrogen dissociation on the clean Pd(100) surface we have recently shown that the results of classical trajectory calculations are closer to the quantum results than the results of quasiclassical calculations.<sup>21,28</sup> In the quasiclassical calculations the zero-point energy of the molecular vibrations in the gas phase is taken into account. However, in all trajectory calculations the zero-point effects of the frustrated translation and rotation of the hydrogen molecule upon dissociative adsorption are not taken into account. Since the zero-point effects of all modes approximately cancel in the system

$\text{H}_2/\text{Pd}(100)$ ,<sup>28</sup> the quasiclassical calculations overestimate the quantum effects because they consider only the promoting effect of the initial zero-point energy in the molecular vibration but not the hindering effect of the zero-point effects of the frustrated rotation and translation.

In recent studies, McCormack and Kroes have shown that for the dissociative adsorption of  $\text{H}_2/\text{Cu}(100)$  quasiclassical trajectory calculations are actually closer to the quantum results than classical trajectory calculations.<sup>29,30</sup> However, the system  $\text{H}_2/\text{Cu}(100)$  is a late barrier system where the initial vibrational energy is very effective in promoting dissociation.<sup>22</sup> Hence it is apparently important to take the contribution of the vibrational zero-point energy into account. The system  $\text{H}_2/\text{S}(2\times 2)/\text{Pd}(100)$ , on the other hand, is an early barrier system.<sup>6,7</sup> As will be shown below, indeed the classical trajectory calculations are more appropriate for this system than the quasiclassical calculations.

Comparing Fig. 1 and Fig. 2, one general trend is obvious. All the classical results are larger than the quantum results, except for energies below the minimum barrier height. An analysis of this behavior shows that it is caused by zero-point effects.<sup>15</sup> At the minimum barrier position the wave function becomes localized in the degrees of freedom perpendicular to the reaction path. This localization leads to quantized state at the barrier position, and these quantized states are associated with zero-point energies. The sum of all zero-point energies increases the effective quantum barrier by 80 meV.<sup>15</sup> Thus in the quantum dynamics particles experience an effectively higher barrier than do the classical particles. Consequently, the quantum sticking probabilities are smaller than the classical ones. This shows that the promoting effect of tunneling is smaller than the suppressing effect of the zero-point vibrations.

Although the effective barrier in the quantum dynamics is effectively larger by 80 meV, the onset of the sticking probabilities on the energy axis are rather similar for quantum and classical particles. It has been shown that this is caused by the fact that for quantum particles steering is already operative for energies at and below the minimum barrier height.<sup>31</sup> This leads to an additional promoting effect in addition to tunneling for the quantum particles.

In Fig. 2 it is obvious that initial vibrational motion of the molecules enhances the sticking probability, as in the quantum calculations. This actually confirms that for this system classical trajectory calculations are more appropriate than quasiclassical calculations, since the quasiclassical sticking probabilities would be even larger than the purely classical ones, which are already larger than the quantum results. However, apart from this general shift, the ordering of the sticking probabilities is the same for the classical and the quantum results; even the relative values are almost the same. This shows that the classical calculations reproduce the dynamical effects of initial vibration and rotation on the sticking probabilities rather well, even for the lightest molecule  $\text{H}_2$ , where the quantum effects are most prominent. Hence for all heavier molecules like  $\text{N}_2$ ,  $\text{O}_2$ ,  $\text{CO}$ , etc., a classical description of the dissociation dynamics should be sufficient.

### B. Dependence of the sticking probability on the angle of incidence

The dependence of the sticking probability on the angle of incidence is related to the corrugation of the potential energy

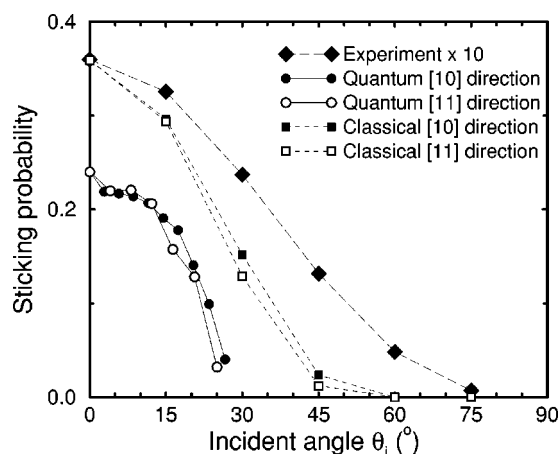


FIG. 3. Sticking probability as a function of the angle of incidence for an initial kinetic energy of 0.4 eV. The diamonds correspond to the experimental results of Ref. 1, which have been scaled by a factor of 10 in order to make the comparison with the calculations easier as far as the relative change is concerned. The circles denote the quantum results while the boxes correspond to the classical results. Results for incidence along the [10] direction of the square unit cells are plotted as filled symbols while open symbols show the results for incidence along the [11] direction, which corresponds to the diagonal of the square surface unit cell.

surface.<sup>32,33</sup> If the surface is not corrugated but perfectly flat, then the sticking probability depends only on the normal component of the kinetic energy of the impinging particle; the system exhibits so-called normal energy scaling. On the other hand, the consequences of corrugation of the surface on the sticking probability are not straightforward. Corrugated surfaces can still show normal energy scaling if the higher energetic barriers are further away from the surface than the lower barriers.<sup>32,33</sup> This scenario is called balanced corrugation.<sup>22</sup>

The  $\text{H}_2/(2\times 2)\text{S}/\text{Pd}(100)$  PES is very strongly corrugated. For molecules with axis parallel to the surface the barrier height to dissociative adsorption varies between 0.09 eV and 2.5 eV within the surface unit cell.<sup>7</sup> Due to this large energetic corrugation we expect that additional parallel momentum will suppress the sticking probability.<sup>32,33</sup>

In Fig. 3 the sticking probability as a function of the angle of incidence is plotted for an initial kinetic energy of 0.4 eV according to the quantum and classical calculations. All the quantum results are smaller than the corresponding classical ones again, due to the zero-point effects which were discussed above. The theoretical results are also compared to the experimental results from Ref. 1, which we have scaled with a factor of 10 in order to make the comparison of the relative variation between experiment and theory easier. Apart from the absolute values, the angular dependence of all three sets of results is rather similar, demonstrating that the variation of the barrier heights close to the minimum barrier of  $\text{H}_2/(2\times 2)\text{S}/\text{Pd}(100)$  is well reproduced by the DFT calculations.

For the experimental results the incident azimuth was not specified. We have determined the theoretical results for two different azimuthal angles, for the beam incident along the [10] direction of the square surface unit cell (filled symbols in Fig. 3) and along the [11] direction, which corresponds to

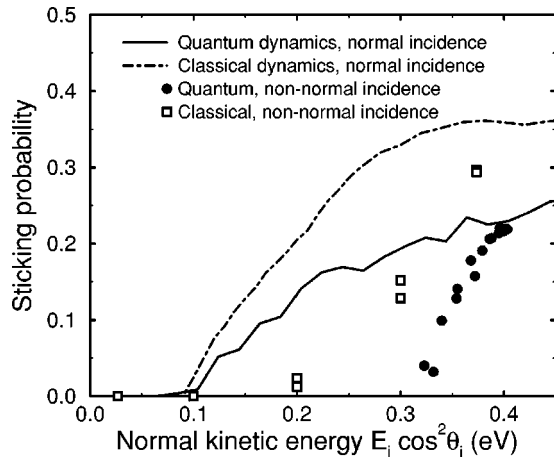


FIG. 4. Calculated sticking probabilities as a function of the normal kinetic energy  $E_i \cos^2 \theta_i$ . The solid and the dot-dashed lines correspond to quantum and classical results for normal incidence, respectively. The dots denote the quantum results for non-normal incidence while the open squares show the classical results. The total kinetic energy for the results for non-normal incidence was  $E_{kin} = 0.4$  eV.

the diagonal of the surface unit cell (open symbols in Fig. 3). It is obvious that the azimuthal dependence of the results is rather weak. At higher angles of incidence the results for the [11] direction are slightly smaller. This can be understood as a shadowing effect. Along this direction the most favorable adsorption site is ‘‘hidden’’ behind a palladium and a sulfur atom, which are both repulsive with respect to hydrogen dissociation. Along the [10] direction there is no such blocking of the most favorable adsorption site, leading to slightly larger sticking probabilities. The effect of the shadowing is relatively small, though, because steering of the molecules to the minimum barrier position is rather effective in this system due to the large corrugation of the PES.<sup>14</sup>

Still, from the angular dependence for one kinetic energy it is not obvious whether normal energy scaling is obeyed in this system. In Fig. 4 we have therefore plotted the theoretical sticking probabilities for normal *and* non-normal incidence as a function of the normal component of the kinetic energy  $E_i \cos^2 \theta_i$ , where  $\theta_i$  is the angle of incidence. It is evident that the sticking probabilities for non-normal incidence are much smaller than the sticking probabilities for normal incidence at the same normal kinetic energy. This means that indeed additional parallel momentum strongly suppresses the sticking probability and that hence normal energy scaling is not obeyed in this system. This is a consequence of the huge energetic corrugation of the potential energy surface.

In the experiment<sup>1</sup> the angular dependence of the sticking probability was also measured for smaller kinetic energies. However, since at these lower kinetic energies the sticking is dominated by defect sites that are not present in our theoretical study, we have not attempted to compare our results to the measurements at those low kinetic energies.

### C. Desorption results

Desorption is the time-reversed process of adsorption. Hence adsorption and desorption are related by the principle

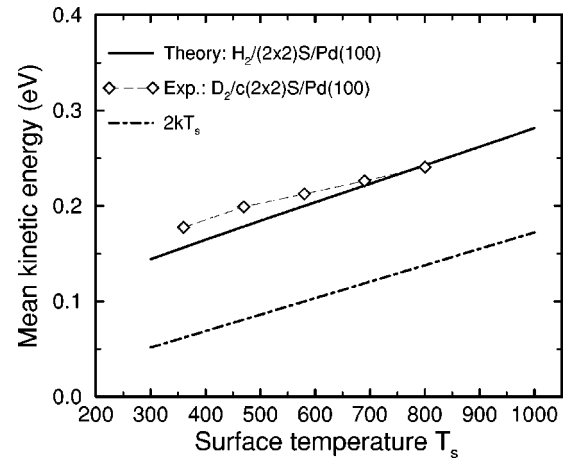


FIG. 5. Mean kinetic energy of hydrogen molecules desorbing from the sulfur-covered Pd(100) surface as a function of the surface temperature. The solid line corresponds to the results from the quantum calculations for  $H_2$  desorbing from  $(2 \times 2)S/Pd(100)$  while the dash-dotted line shows the results expected for a gas at thermal equilibrium with the surface temperature. The experimental results (diamonds) were obtained for  $D_2$  desorbing from  $c(2 \times 2)S/Pd(100)$  (from Ref. 16).

of microscopic reversibility or detailed balance. The distribution of the kinetic and internal energy of desorbing molecules thus reflects the dependence of the sticking probability on the kinetic energy and the internal degrees of freedom, respectively. Whenever the sticking probability increases with increasing energy in one particular mode, e.g., translational or internal energy, then the mean energy in this mode in desorption will be larger than expected for a gas in thermal equilibrium with the surface temperature. This mode is said to be heated in desorption.

The adsorption in the system  $H_2/(2 \times 2)S/Pd(100)$  is activated, i.e., the sticking probability rises with increasing kinetic energy. Consequently, the kinetic energy of  $H_2$  molecules desorbing from the surface at a surface temperature of  $T_s$  should be larger than the flux-weighted thermal equilibrium value of  $2k_B T_s$ . This higher kinetic energy in desorption can also be understood by the argument that the desorbing molecules should in addition to the thermal energy also gain energy that corresponds to the minimum adsorption barrier. Such an argument is only valid, however, if the substrate degrees of freedom are not crucially involved in the desorption process.<sup>34,35</sup>

In Fig. 5 we have compared our calculated mean kinetic energy in desorption with the mean value for a thermal gas at equilibrium as a function of the surface temperature. The calculated results are obtained by invoking time reversal and populating the molecular states with a Boltzmann distribution at the surface temperature. Indeed, the calculated mean kinetic energy is larger than the thermal value by approximately 0.1 eV, which is close to the minimum barrier height of 0.09 eV.

Furthermore, in Fig. 5 we have plotted experimental results for the desorption of  $D_2$  from  $c(2 \times 2)S/Pd(100)$  obtained by time-of-flight (TOF) measurements.<sup>16</sup> These results compare quite well with our calculations. This comparison should be done with caution since, first, in the experiment a different isotope has been used and, second, the molecules

were desorbed from a Pd surface with a higher sulfur coverage than in the calculations. However, the experimentalists had checked for an isotope effect, and within the experimental uncertainties they could not detect any.<sup>16</sup>

As for the sulfur coverage, according to DFT calculations<sup>7</sup> hydrogen dissociation at the  $c(2\times 2)$  sulfur-covered Pd(100) surface corresponding to a sulfur coverage of  $\Theta_S=0.5$  should be hindered by energetic barriers larger than 2 eV. Consequently, hydrogen molecules desorbing from such a surface should have an excess energy of more than 2 eV. Now there are still uncertainties with respect to the functionals in the GGA-DFT calculations (see, e.g., Ref. 36); however, an error of 2 eV is not to be expected. Hydrogen molecules desorbing from a sulfur-covered surface at a sulfur coverage of  $\Theta_S=0.5$  with such a high excess energy have not been observed. This indicates that indeed the hydrogen molecules are desorbing from parts of the surface where locally the sulfur coverage is lower than  $\Theta_S=0.5$ . The huge calculated barriers for hydrogen dissociation at the  $c(2\times 2)$  sulfur-covered Pd(100) surface are in fact in agreement with the experimental results of Burke and Madix,<sup>2</sup> who found that for sulfur coverages above  $\Theta_S=0.28$  no hydrogen dissociation on Pd(100) is possible.

This reasoning is actually also supported by the TOF measurements.<sup>16</sup> The kinetic energy in desorption was measured for a range of sulfur coverages from  $\Theta_S=0.15$  to  $\Theta_S=0.5$  for a surface temperature of  $T_s=500$  K. For all these sulfur coverages a slow and a fast component have shown up in the TOF spectra, where the slow component corresponds to molecules desorbing from surface sites without an adsorption barrier, while the fast component (which is plotted in Fig. 5) was almost independent of the sulfur coverage. This indicates that the sulfur overlayer was not very well ordered so that there were surface regions which were almost sulfur-free while others had a high local sulfur coverage. Because of the independence of the fast TOF component of the sulfur coverage, it is reasonable to attribute this fast component to molecules desorbing from a locally ordered  $(2\times 2)$  sulfur overlayer. Hence the comparison between our calculations and the experiment is meaningful.

Finally we turn to the rotational alignment of desorbing hydrogen molecules. As shown in Fig. 1, molecules rotating in the so-called helicopter fashion have a higher sticking probability than molecules rotating in the cartwheel fashion. Again invoking the principle of detailed balance, this means that in desorption the rotating molecules should preferentially rotate in the helicopter fashion.

This alignment can actually be measured by laser-induced fluorescence (LIF).<sup>37</sup> In Fig. 6 is plotted the rotational alignment parameter  $A_0^{(2)}(j)$  which is given by

$$A_0^{(2)}(j) = \left\langle \frac{3J_z^2 - \mathbf{J}^2}{\mathbf{J}^2} \right\rangle_j. \quad (1)$$

$A_0^{(2)}(j)$  corresponds to the quadrupole moment of the orientational distribution and assumes values of  $-1 \leq A_0^{(2)}(j) \leq 2$ . Molecules rotating preferentially in the cartwheel fashion have an alignment parameter  $A_0^{(2)}(j) < 0$ ; for molecules rotating preferentially in the helicopter fashion  $A_0^{(2)}(j) > 0$ .

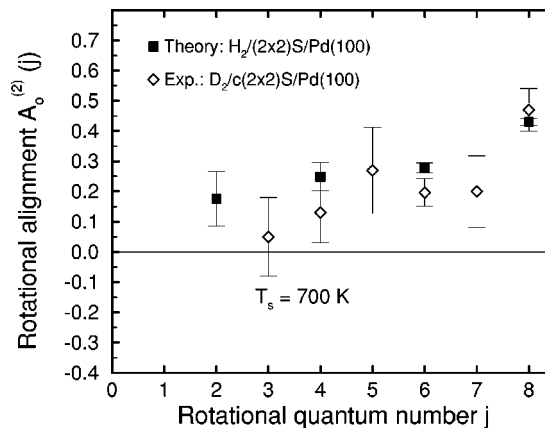


FIG. 6. Rotational alignment of hydrogen molecules desorbing from the sulfur-covered Pd(100) surface at a surface temperature of  $T_s=700$  K. The squares show the calculated quantum results for  $H_2$  desorbing from  $(2\times 2)S/Pd(100)$  while the diamonds denote the experimental results of  $D_2$  desorbing from  $c(2\times 2)S/Pd(100)$  (from Ref. 17).

Converged results for the sticking probability as a function of the kinetic energy have been calculated in quantum dynamics for rotational quantum numbers up to  $j=8$ . This allows determination of the theoretical rotational alignment in desorption by invoking time reversal. However, the *ab initio* results for the PES have been fitted to an analytical form that allows only transitions between rotational states with  $\Delta m_j$  even, where  $m_j$  is the azimuthal quantum number.<sup>7</sup> Reaction probabilities have been determined only for states with even rotational and azimuthal quantum numbers  $j$  and  $m_j$ , respectively. Hence the results for odd  $m_j$  which enter the determination of the rotational alignment parameter in Eq. (1) had to be estimated, which was simply done by a linear interpolation. This is the reason why the theoretical results in Fig. 6 are plotted with error bars.

Again the comparison between theoretical and experimental results in Fig. 6 should be done with caution because the theoretical results have been obtained for  $H_2$  desorbing from  $(2\times 2)S/Pd(100)$  while the experimental results have been measured for  $D_2$  desorbing from  $c(2\times 2)S/Pd(100)$ .<sup>17</sup> As for the isotope effect, at the clean surface the rotational alignment of  $H_2$  and  $D_2$  desorbing from Pd(100) does not differ within the experimental uncertainties,<sup>38,39</sup> hence we expect a vanishing isotope effect with respect to the rotational alignment also for the sulfur-covered surface. This is actually reasonable because the velocity of  $H_2$  and  $D_2$  and their speed of rotation scale exactly in the same way with their masses at a given kinetic energy. For the rotational quantum number  $j=8$  the dependence of the rotational alignment on the sulfur coverage has actually been measured.<sup>17</sup> Between  $\Theta_S=0.25$  and  $\Theta_S=0.5$  the rotational alignment did not depend on the actual sulfur coverage. Assuming that the same is true for the other rotational quantum numbers, the comparison of theoretical and experimental results in Fig. 6 is justified. This comparison demonstrates that within the experimental and theoretical uncertainties the measured and calculated values for the rotational alignment agree quite well. Again this shows that the most favorable reaction path is well described by our *ab initio* quantum molecular dynamics calculations.

The results of Fig. 6 confirm that molecules rotating in the helicopter fashion have indeed a higher dissociation probability than molecules rotating in the cartwheel fashion because all measured and calculated alignment factors are larger than zero. The general trend is an increase in the alignment factor with increasing rotational quantum number. This behavior has also been found for other activated dissociative adsorption systems, theoretically<sup>40</sup> for  $\text{H}_2/\text{Ag}(100)$  and experimentally<sup>41</sup> for  $\text{D}_2/\text{Cu}(111)$  [although other experiments<sup>42</sup> report a vanishing alignment for  $\text{D}_2/\text{Cu}(111)$ ]. This can simply be understood by the fact that for higher  $j$  the  $m_j = j$  state becomes more and more helicopterlike so that the steric preference becomes larger. However, for hydrogen desorbing from the clean  $\text{Pd}(100)$  surface experiments show a positive alignment factor for  $j \leq 6$  but for  $j \geq 7$  the alignment becomes basically zero.<sup>38,39</sup> This behavior is still not completely understood.

## V. CONCLUSIONS

In conclusion, we reported a six-dimensional dynamical study of the dissociative adsorption of  $\text{H}_2$  at  $\text{S}(2 \times 2)/\text{Pd}(100)$  employing a PES obtained from detailed density-functional theory calculations. The dynamical results reproduce the poisoning effect of sulfur adsorption for hydrogen dissociation on  $\text{Pd}(100)$ , but large quantitative differences from experiment exist, as far as the absolute value of the sticking coefficient is concerned.

However, the relative change of the sticking coefficient as a function of the angle of incidence found in experiment is well reproduced by the calculations. In addition, the measured mean kinetic energy and the rotational alignment of  $\text{D}_2$  desorbing from the  $c(2 \times 2)$  sulfur-covered  $\text{Pd}(100)$  surface are in good agreement with our calculations for  $\text{H}_2$  desorbing from the  $(2 \times 2)$  sulfur-covered  $\text{Pd}(100)$  surface. All these results together indicate that the minimum energy barrier as well as the corrugation and anisotropy of the potential energy surface close to the most favorable reaction path are well

reproduced by the calculations. They further suggest that the quantitative differences between theory and experiment are related to uncertainties in the preparation and determination of the experimental sulfur overlayer.

According to *ab initio* total-energy calculations, hydrogen molecules desorbing from the  $c(2 \times 2)$  sulfur-covered  $\text{Pd}(100)$  surface should have an excess energy of more than 2 eV, which is ten times larger than what is observed in experiment. We therefore propose that the sulfur-covered  $\text{Pd}$  samples used in the experiments were probably not very well ordered, so that the measured desorption events correspond to molecules desorbing from local  $(2 \times 2)$  sulfur structures. In the molecular beam adsorption experiment the sulfur adlayer was produced by segregation of bulk sulfur. Hence subsurface sulfur might well have been present in the experimental sample, while the calculations considered only a pure sulfur adlayer without any subsurface sulfur. This might be an additional reason for the difference between experiment and theory.

In order to understand the differences between experiment and theory it is certainly desirable that in addition to further theoretical studies more detailed experiments on the dynamics of hydrogen adsorption at and desorption from sulfur-covered surfaces under well-defined conditions should be performed. If the discrepancies between theory and experiment that we have identified above persist in these cases, important questions associated with the underlying theory will be raised.

## ACKNOWLEDGMENTS

We wish to thank D. Wetzig, M. Rutkowski, and H. Zacharias for providing us with their results prior to publication. In addition, we gratefully acknowledge useful discussions with them. Special thanks go to Jakob Pichlmeier for creating the massively parallel version of the coupled-channel scheme.

<sup>1</sup>K. D. Rendulic, G. Anger, and A. Winkler, *Surf. Sci.* **208**, 404 (1989).

<sup>2</sup>M.L. Burke and R.J. Madix, *Surf. Sci.* **237**, 1 (1990).

<sup>3</sup>J.A. Rodriguez, T. Jirsak, and S. Chaturvedi, *J. Chem. Phys.* **110**, 3138 (1999).

<sup>4</sup>P.J. Feibelman and D.R. Hamann, *Phys. Rev. Lett.* **52**, 61 (1984).

<sup>5</sup>S. Wilke and M. Scheffler, *Surf. Sci.* **329**, L605 (1995).

<sup>6</sup>S. Wilke and M. Scheffler, *Phys. Rev. Lett.* **76**, 3380 (1996).

<sup>7</sup>C.M. Wei, A. Groß, and M. Scheffler, *Phys. Rev. B* **57**, 15 572 (1998).

<sup>8</sup>D.M. Bird, *Faraday Discuss.* **110**, 335 (1998).

<sup>9</sup>P.A. Grivil and H. Toulhoat, *Surf. Sci.* **430**, 176 (1999).

<sup>10</sup>B. Hammer and J.K. Nørskov, *Surf. Sci.* **343**, 211 (1995).

<sup>11</sup>S. Wilke, M. Cohen, and M. Scheffler, *Phys. Rev. Lett.* **77**, 1560 (1996).

<sup>12</sup>J.K. Nørskov, S. Holloway, and N.D. Lang, *Surf. Sci.* **137**, 65 (1984).

<sup>13</sup>A. Eichler, J. Hafner, A. Groß, and M. Scheffler, *Phys. Rev. B* **59**, 13 297 (1999).

<sup>14</sup>A. Groß, *Surf. Sci. Rep.* **32**, 291 (1998).

<sup>15</sup>A. Groß, C.M. Wei, and M. Scheffler, *Surf. Sci.* **416**, L1095 (1998).

<sup>16</sup>G. Comsa, R. David, and B.-J. Schumacher, *Surf. Sci.* **95**, L210 (1980).

<sup>17</sup>M. Rutkowski, D. Wetzig, and H. Zacharias (unpublished).

<sup>18</sup>J. P. Perdew, J. A. Chevary, S. H. Vosko, K. A. Jackson, M. R. Pederson, D. J. Singh, and C. Fiolhais, *Phys. Rev. B* **46**, 6671 (1992).

<sup>19</sup>W. Brenig, T. Brunner, A. Groß, and R. Russ, *Z. Phys. B: Condens. Matter* **93**, 91 (1993).

<sup>20</sup>W. H. Press, B. P. Flannery, S. A. Teukolsky, and W. T. Vetterling, *Numerical Recipes* (Cambridge University Press, Cambridge, 1989).

<sup>21</sup>A. Groß and M. Scheffler, *Phys. Rev. B* **57**, 2493 (1998).

<sup>22</sup>G. R. Darling and S. Holloway, *Rep. Prog. Phys.* **58**, 1595 (1995).

<sup>23</sup>Axel Groß, *Phys. Status Solidi B* **217**, 389 (2000).

<sup>24</sup>W. Berndt, R. Hora, and M. Scheffler, *Surf. Sci.* **117**, 188 (1982).

<sup>25</sup>M. Rutkowski (private communication).

- <sup>26</sup>A. Groß, S. Wilke, and M. Scheffler, Phys. Rev. Lett. **75**, 2718 (1995).
- <sup>27</sup>J. C. Polanyi and W. H. Wong, J. Chem. Phys. **51**, 1439 (1969).
- <sup>28</sup>A. Groß and M. Scheffler, J. Vac. Sci. Technol. A **15**, 1624 (1997).
- <sup>29</sup>D. A. McCormack and G. J. Kroes, Chem. Phys. Lett. **296**, 515 (1998).
- <sup>30</sup>D. A. McCormack and G. J. Kroes, Phys. Chem. Chem. Phys. **1**, 1359, 1999.
- <sup>31</sup>A. Groß, J. Chem. Phys. **110**, 8696 (1999).
- <sup>32</sup>G.R. Darling and S. Holloway, Surf. Sci. **304**, L461 (1994).
- <sup>33</sup>A. Groß, J. Chem. Phys. **102**, 5045 (1995).
- <sup>34</sup>W. Brenig, A. Groß, and R. Russ, Z. Phys. B: Condens. Matter **96**, 231 (1994).
- <sup>35</sup>A. Groß, M. Bockstedte, and M. Scheffler, Phys. Rev. Lett. **79**, 701 (1997).
- <sup>36</sup>B. Hammer, L. B. Hansen, and J. K. Nørskov, Phys. Rev. B **59**, 7413 (1999).
- <sup>37</sup>D. Wetzig, R. Dopheide, R. David, and H. Zacharias, Ber. Bunsenges. Phys. Chem. **99**, 1353 (1995).
- <sup>38</sup>D. Wetzig, R. Dopheide, M. Rutkowski, R. David, and H. Zacharias, Phys. Rev. Lett. **76**, 463 (1996).
- <sup>39</sup>D. Wetzig, M. Rutkowski, W. Etterich, R. David, and H. Zacharias, Surf. Sci. **402**, 232 (1998).
- <sup>40</sup>A. Eichler, J. Hafner, A. Groß, and M. Scheffler, Chem. Phys. Lett. **311**, 1 (1999).
- <sup>41</sup>S.J. Gulding, A. M. Wodtke, H. Hou, C. T. Rettner, H. A. Michelson, and D. J. Auerbach, J. Chem. Phys. **105**, 9702 (1996).
- <sup>42</sup>D. Wetzig, M. Rutkowski, R. David, and H. Zacharias, Europhys. Lett. **36**, 31 (1996).